Inorganic Chemistry

ARTICLE

pubs.acs.org/IC

Condensed Tantalaborane Clusters: Synthesis and Structures of $[(Cp^*Ta)_2B_5H_7\{Fe(CO)_3\}_2]$ and $[(Cp^*Ta)_2B_5H_9\{Fe(CO)_3\}_4]$

Shubhankar Kumar Bose,[†] K. Geetharani,[†] Babu Varghese,[‡] and Sundargopal Ghosh*[,†]

[†]Department of Chemistry and [‡]Sophisticated Analytical Instruments Facility, Indian Institute of Technology Madras, Chennai 600 036, India

Supporting Information

ABSTRACT:

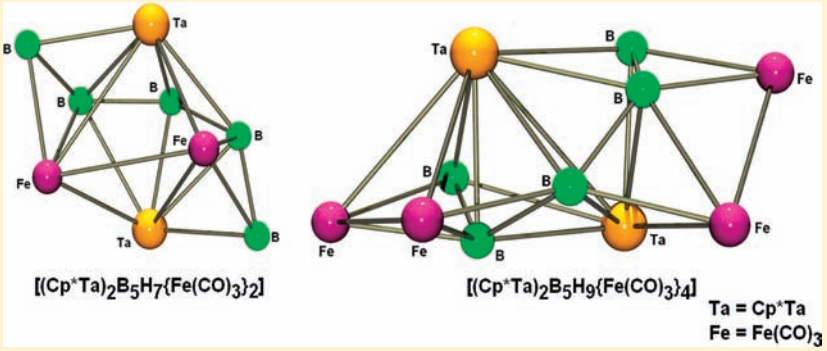

The reaction of $[(Cp^*Ta)_2B_4H_9(\mu\text{-}BH_4)]$ (**1**; $Cp^* = \eta^5\text{-}C_5Me_5$) with $[Fe_2(CO)_9]$ in hexane yielded $[(Cp^*Ta)_2B_5H_7\{Fe(CO)_3\}_2]$ (**2**) and $[(Cp^*Ta)_2B_5H_9\{Fe(CO)_3\}_4]$ (**3**) in moderate yield. Cluster **2** represents the first example of a bicapped pentagonal-bipyramidal metallaborane with a deformed equatorial plane, and **3** can be described as a fused cluster in which two pentagonal-bipyramidal units are fused through a common 3-vertex triangular face. Compounds **2** and **3** have been characterized by mass spectrometry and IR, ^1H, ^{11}B, and ^{13}C NMR spectroscopy, and the geometric structures were unequivocally established by crystallographic analysis.

INTRODUCTION

Metallaborane cage chemistry is an interesting and increasingly developing field of study.[1,2] There are a very large number of metallaborane compounds known, and the electron-counting rules plus the isolobal principle provide a solid foundation for understanding the interrelationships between the structure and composition.[3,4] Conventionally, there are three complementary approaches to the expansion of cluster networks containing transition-metal fragments:[1,5] (i) condensation involving monoborane reagents, (ii) insertion or fragmentation involving borane or metal carbonyl fragments, and (iii) intercluster fusion with two or more atoms held in common between the constituent subclusters. In each case, reaction often leads to the formation of a wide range of products with different metal-to-boron ratios.[6]

In recent years, we have been exploring the reactions of monocyclopentadienylmetal chloride with monoborane reagents (e.g., $BH_3\cdot$THF and $LiBH_4\cdot$THF, where THF = tetrahydrofuran) as a general route to dimetallaboranes. As a result, we have made several novel metallaboranes, in which some of them showed interesting reaction chemistry.[7−10] The reactions of transition-metal fragment sources with metal clusters generally result in metal fragment substitutions or additions.[11,12] Although less studied, the same is true of such reactions involving metallaboranes.[13−15] Hence, we have investigated the reaction of $[(Cp^*Ta)_2B_4H_9(\mu\text{-}BH_4)]$ (**1**) with $[Fe_2(CO)_9]$, which generated $[(Cp^*Ta)_2B_5H_7\{Fe(CO)_3\}_2]$ (**2**) and $[(Cp^*Ta)_2B_5H_9\{Fe(CO)_3\}_4]$ (**3**). Reported here are the synthesis and structural characterization of two novel 9- and 11-vertex clusters.

RESULTS AND DISCUSSION

Mild pyrolysis of **1** with $[Fe_2(CO)_9]$ in hexane generated **2** and **3**, in parallel with the formation of a μ_3-borylene complex, $[(\mu_3\text{-}BH)(Cp^*TaCO)_2(\mu\text{-}CO)\{Fe(CO)_3\}]$[7c] (Scheme 1). This reaction also produced other products, which were observed during the chromatographic workup, but because of instability and insufficient amounts, isolation and characterization were not possible. Although compounds **2** and **3** are produced in a mixture, these compounds can be separated by preparative thin-layer chromatography (TLC), allowing characterization of pure materials. Descriptions of the characterization of **2** and **3** from mass spectrometry, IR, NMR, and X-ray diffraction studies follow.

The molecular structure of **2**, shown in Figure 1, reveals that the cage geometry is based on a pentagonal bipyramid with two additional boron vertices capping its two trigonal faces. The iron

Received: November 8, 2010
Published: February 22, 2011

Scheme 1. Synthesis of 2, 3, and a Triply Bridged Borylene Complex, $[(\mu_3\text{-BH})(Cp^*TaCO)_2(\mu\text{-CO})\{Fe(CO)_3\}]$[a]

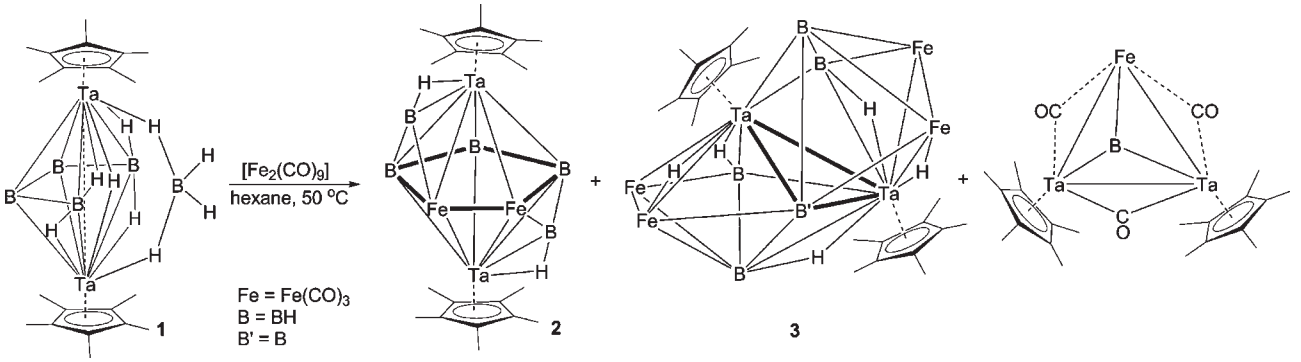

[a] Antipodal Ta−B bonds of **3** are not shown for clarity.

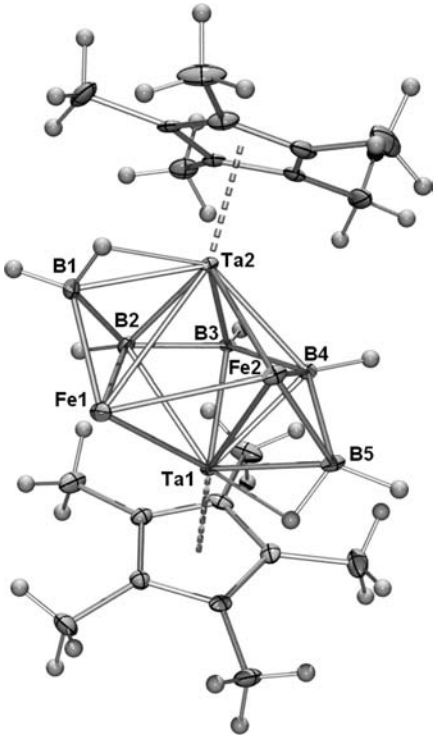

Figure 1. Molecular structure and labeling diagram for **2**. Terminal carbonyl ligands are excluded for clarity. Thermal ellipsoids are shown at the 50% probability level. Selected bond lengths (Å) and angles (deg): Fe1−Fe2 2.9207(7), Ta1−Fe1 2.5189(5), Ta1−Fe2 3.0008(5), Ta2−Fe1 3.0123(5), Ta2−Fe2 2.5330(5), Fe2−B4 2.237(4), Fe1−B2 2.243(4), B2−B3 1.757(5), B3−B4 1.764(5), Ta2−B2 2.258(4), Ta2−B3 2.231(4), Ta2−B4 2.462(4), Ta1−B2 2.473(4), Ta1−B3 2.241(4), Ta1−B4 2.271(4), Ta2−B1 2.254(4), Fe1−B1 2.161(4), B1−B2 1.748(6); B2−Fe1−Fe2 89.21(10), B2−B3−B4 120.6(3), B4−Fe2−Fe1 89.33(9), Fe1−B1−Ta2 86.01(14), B2−B1−Ta2 67.32(18).

atoms Fe1 and Fe2 and the three boron atoms B2, B3, and B4 define the pentagonal plane, while the tantalum atoms Ta1 and Ta2 occupy the apical positions. In addition, two boron atoms, B1 and B5, bridge the triangular faces Fe1−B2−Ta2 and Fe2−B4−Ta1, respectively. Metallaheptaboranes containing pentagonal-bipyramidal geometry are rare, and very few examples are known, for example, $[B_6H_6Cp^*Ni]^{2-}$,[16] $[B_5H_7(Cp^*Co)_2]$,[17] and *closo*-$[B_5H_4PPh_3\{Fe(CO)_3\{Ir(CO)_2PPh_3\}]$.[18] Among these, *closo*-$[B_5H_4PPh_3\{Fe(CO)_3\{Ir(CO)_2PPh_3\}]$ is the first structurally characterized pentagonal-bipyramidal metallaborane in which the $[Fe(CO)_3]^{2+}$ vertex caps a formal *nido*-$[B_5H_4(PPh_3)\{Ir(CO)_2(PPh_3)\}]^{2-}$ unit. Similarly, the first boron-capped pentagonal-bipyramidal metallacarborane, $[(Ph_3P)_2HRuCB_6H_4(OMe)_3]$, was isolated from the reaction of $[nido\text{-}B_{10}H_{12}CH]^-Cs^+$ with $[RuCl_2(PPh_3)_3]$.[19] More recently, Fehlner and co-workers have reported the bimetallacarborane $[Cp^*Ir(B_3H_3C_2Me_2)\{Mo(CO)_3\}(\mu\text{-CO})]$,[20] which also has similar geometry.

The apical Ta−Ta separation in **2** (3.441 Å) is significantly longer than that found in **1** [2.8946(2) Å].[7b] The Ta−$B_{equatorial}$ distances of 2.241−2.473 Å, similar to or longer than the Fe−$B_{equatorial}$ distances of 2.172 and 2.237 Å, perhaps reflect the η^5 coordination of the tantalum. Similarly, the $B_{equatorial}$−$B_{capping}$ distances (1.741 and 1.748 Å) are slightly shorter than the equatorial belt distances (1.757 and 1.768 Å). The Fe1−Fe2 distance in the pentagon is 2.921 Å, while the internal angles within this pentagon are in the range of 89.21(10)−120.65(2)° (105.70° average), less than the expected value (108°) for a planar structure.[21] Indeed, the equatorial Fe1−B2−B3−B4−Fe2 ring is not in the plane; this may be due to the longer metal−metal bonds in the cluster [Ta1−Fe2 = 3.0008(5) Å and Ta2−Fe1 = 3.0123(5) Å].

Consistent with the X-ray results, the ^{11}B NMR spectrum of **2** rationalizes the presence of three boron resonances in the ratio of 2:2:1, which collapsed into sharp singlets upon broad-band ^1H decoupling, indicating one terminal hydrogen atom on each boron atom. The signal at $\delta(^{11}B)$ = 84.7 ppm is tentatively assigned to the unique boron of the pentagonal plane. The other two resonances of relative intensity 2:2 at $\delta(^{11}B)$ = 53.9 and 36.5 ppm can be assigned to the capping boron atoms and cage boron atoms, respectively. The ^1H and ^{13}C NMR spectra of **2**, measured at room temperature, are consistent with its symmetrical structure. In particular, ^1H NMR data reveal the presence of one kind of Cp* signal and one signal for two Ta−H−B protons. The IR spectrum in the carbonyl region shows three terminal carbonyl frequencies at 2024, 1996, and 1966 cm^{-1}, which are assigned to $Fe(CO)_3$ fragments, and bands at 2510 and 2498 cm^{-1}, owing to the terminal B−H stretches.

Compound **3** was isolated in 14% yield as a red-brown solid. Single crystals suitable for X-ray diffraction analysis of **3** were obtained from a hexane solution at −10 °C, thus allowing for the structural characterization of cluster **3**. The crystal structure showed hexane of solvation and contains two independent molecules in the asymmetric unit. A solid-state structure of one

dx.doi.org/10.1021/ic102235p |*Inorg. Chem.* 2011, 50, 2445–2449

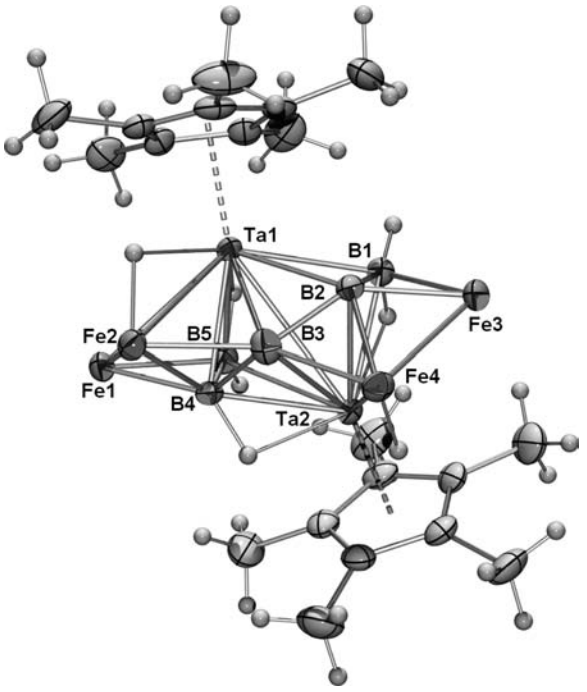

Figure 2. Molecular structure and labeling diagram for **3**. Terminal carbonyl ligands are excluded for clarity. Thermal ellipsoids are shown at the 40% probability level. Selected bond lengths (Å) and angles (deg): Ta1−Ta2 3.280, B4−Ta1 2.351(6), Fe1−Fe2 2.6603(12), Fe1−Ta1 2.9155(9), Fe2−Ta1 2.8456(9), B3−Ta1 2.315(7), B5−Ta1 2.310(6), B5−Ta2 2.554(6), B3−Ta2 2.464(6), B4−B5 1.736(9), B3−B4 1.828(9), B4−Fe1 2.026(6), B4−Fe2 2.187(6), Fe3−Fe4 2.6719(12), B1−Ta1 2.533(6), Fe3−Ta2 2.9644(9), B2−B3 1.683(9); B5−Fe1−Fe2 96.81(17), Fe1−B5−Ta2 123.7(3), B3−Ta2−B5 77.0(2), Fe2−B3−Ta2 130.6(3), Fe4−Ta2−Fe3 54.48(2), Fe2−Ta1−Fe1 54.99(2), Fe4−B2−Ta1 132.7(3).

of the two independent molecules in the crystal of **3** is shown in Figure 2. The observed geometry of **3** can be viewed as a 7-vertex nido species (Ta_2B_5 unit) formally derived from an 8-vertex closo hexagonal-bipyramidal cluster by removal of one equatorial vertex, in which two of the TaB_2 faces symmetrically capped by $Fe(CO)_3$ groups. The resulting two FeB_2 faces are, in turn, capped by two other $Fe(CO)_3$ groups, thereby generating a overall tetracapped nido structure **3**. Alternatively, cluster **3** may be considered as a fused cluster, generated from the fusion of two 7-vertex *closo*-$\{Ta_2Fe_2B_3\}$ units with three atoms held common between the two subclusters. The equatorial belt of the pentagonal bipyramid in one of the subclusters consists of Fe1, Fe2, B3, Ta2, and B5 atoms, whereas Ta1 and B4 are present in apical positions. Similarly, Fe3, Fe4, B3, Ta1, and B1 define the pentagonal plane, while Ta2 and B2 occupy the apical positions in another subcluster. Although all of the BH terminal protons were not located in the X-ray diffraction study, evidence for their presence has been supported by the $^1H\{^{11}B\}$ NMR spectrum.

The Ta−Ta distance (Ta1−Ta2 3.280 Å) is too long for a full Ta−Ta single bond (cf. $[(Cp^*TaCl)_2B_5H_{11}]$[7a]), but it is too short to propose that there is no significant interaction at all between the two metal centers.[22] Two of the metal−metal bonds, Fe1−Ta1 2.9155(9) Å and Fe3−Ta2 2.9644(9) Å, in **3** are unusually long. A similar distortion in the metal−metal bonding was also observed in the complex $[Ru_6(CO)_{13}(\mu\text{-}MeC_2NMe_2)(\mu_3\text{-}MeC_2NMe_2)(\mu_4\text{-}S)_2]$, which contains a Ru_5S_2 cluster core with pentagonal-bipyramidal geometry.[23] On the other hand, the hydrogen-bridged Fe−Ta bond distances [Fe2−Ta1 2.8456(9) Å and Fe4−Ta2 2.8701(9) Å] are significantly shorter compared to other Fe−Ta distances. The Fe−Fe separations appear normal for the pentagonal-bipyramidal cage structure and can be compared with $[(R'P)(RCCR)Fe_4(CO)_{11}]$ (R′ = ^{t}Bu and R = Ph).[24] The shortest B(apical)−B(basal) edge is B2−B3, which is 1.683(9) Å, while the other B−B distances range from 1.720(9) to 1.828(9) Å. As illustrated in Figure 2, the two pentagonal planes are far from ideal. The Fe4−B3−Ta1 and Fe2−B3−Ta2 angles of 138.5° and 130.6°, respectively, are larger, and the angles B3−Ta1−B1 and B3−Ta2−B5 of 77.6° and 76.97°, respectively, are far less than the ideal pentagonal angle of 108°.

Chart 1. Fused Pentagonal Bipyramidal Clusters[a]

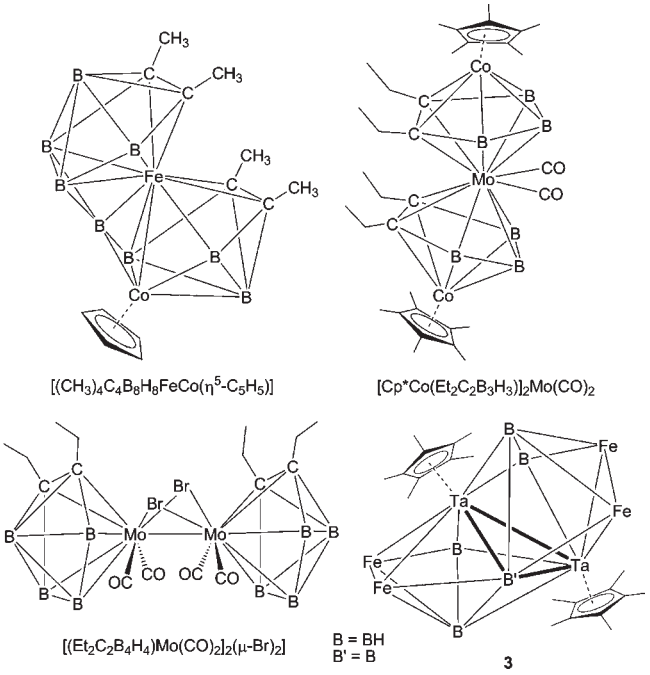

[a]Antipodal Ta−B bonds and the bridging hydrogen atoms of **3** are not shown for clarity.

The ^1H and ^{11}B NMR spectra are consistent with the solid-state X-ray structure of **3**, which rationalizes the presence of five ^{11}B resonances with equal intensity. Besides the BH terminal protons, two Ta−H−Fe and three Ta−H−B (1:1:1) protons were also observed. Furthermore, ^1H and ^{13}C NMR spectra imply two equivalent Cp* ligands. The parent ion of **3** in the mass spectrum fragments by the sequential loss of 12 CO molecules, and the molecular mass corresponds to $Cp^*_2Ta_2Fe_4(CO)_{12}B_5H_9$. The IR spectrum shows three terminal carbonyl frequencies at 2032, 1994, and 1938 cm^{-1}, and the band at 2489 cm^{-1} is due to the terminal B−H.

The geometry of cluster **3** is unusual. There are only few crystallographically characterized clusters known in which two pentagonal-bipyramidal units are fused via a vertex (Chart 1), for example, bimetallacarboranes $[Me_4C_4B_8H_8FeCo(Cp)]$[25] and $[Me_4C_4B_8H_8FeCo(PEt_3)_2]$[26] consisting of two fused 7-vertex closo pentagonal-bipyramidal polyhedra with the unique boron atom wedged between both cages. Another small metallacarborane dimer is $[(Et_2C_2B_4H_4)Mo(CO)_2]_2(\mu\text{-}Br)_2]$, in which two MC_2B_4 pentagonal-pyramidal clusters are linked via an intercluster

dx.doi.org/10.1021/ic102235p |*Inorg. Chem.* 2011, 50, 2445–2449

metal−metal bond. Further, the bent-tetradecker sandwich cluster $[Cp^*Co(Et_2C_2B_3H_3)]_2Mo(CO)_2$, reported by Grimes, was the first of its type in metallacarborane chemistry.[27] As far as we are aware, compound **3** is the first known example of a face fusion of two pentagonal-bipyramidal units.

Following the skeletal electron-counting rules,[3,28] cluster **2** has 12 skeletal electrons, i.e., 8 electrons less than expected for a normal 9-vertex closo cluster. Therefore, cluster **2** can be considered as a hyper-*closo*-metallaborane. Distortion of the standard deltahedron for a given closo *n*-atom skeleton to that observed leads to a reduced number of low-energy cluster bonding orbitals, thereby supporting the low skeletal electron pair (sep) count found. Alternatively, on the basis of the capping principal,[29,30] the skeletal electron count is determined by the central polyhedron (i.e., $Ta_2Fe_2B_3$ pentagonal bipyramid in **2**), which amounts to six sep's, two less than what was required for the bicapped pentagonal-bipyramidal geometry. Thus, neither the capping nor the cluster-fusion principles account for the structure of **2**. On the other hand, the cluster **3** appears to follow the regular electron-counting rules because it possesses nine sep's appropriate for a normal 7-vertex nido cluster. The total valence electron count of 100 for cluster **3** can be further rationalized using Mingos fusion formalism.[29b−d]

CONCLUSION

The metallaboranes **2** and **3** reported here represent a novel class of condensed clusters synthesized from mild pyrolysis of **1** and $[Fe_2(CO)_9]$. Up to now, most of the boron-containing capped closo clusters are bimetalla- or trimetallaboranes based on a capped octahedron, in which a BH or a metal-containing group caps one of the cluster faces.[31] The structure of **2** provides the first and a unique example of a bicapped *closo*-metallaborane based on pentagonal-bipyramidal geometry. Further, the formation of face-fused pentagonal-bipyramidal cluster **3** from **1** appears to be unprecedented.

EXPERIMENTAL SECTION

General Procedures and Instrumentation. All of the operations were conducted under an Ar/N_2 atmosphere using standard Schlenk techniques or a glovebox. Solvents were distilled prior to use under argon. $[Cp^*TaCl_4]$, $[BH_3\cdot THF]$, $[LiBH_4\cdot THF]$, and $[Fe_2(CO)_9]$ (Aldrich) were used as received. $[(Cp^*Ta)_2B_4H_9(\mu\text{-}BH_4)]$ (**1**) was prepared as described in the literature.[7b] The external reference for the ^{11}B NMR spectra, $[Bu_4N(B_3H_8)]$, was synthesized with the literature method.[32] TLC was carried out on 250-mm-diameter aluminum-supported silica gel TLC plates (Merck TLC plates). NMR spectra were recorded on 400 and 500 MHz Bruker FT-NMR spectrometers. Residual solvent protons were used as references (δ, ppm, $[D_6]$benzene, 7.16), while a sealed tube containing $[Bu_4N(B_3H_8)]$ in $[D_6]$benzene (δ_B, ppm, −30.07) was used as an external reference for the ^{11}B NMR spectra. IR spectra were recorded on a Nicolet 6700 FT spectrometer. Microanalyses for C, H, and N were performed on Perkin Elmer Instruments series II model 2400. Mass spectra were obtained on a Jeol SX 102/Da-600 mass spectrometer with argon/xenon (6 kV and 10 mA) as the fast atom bombardment (FAB) gas.

Synthesis of 2 and 3. To a 100 mL Schlenk tube, containing 0.06 g of **1** (0.09 mmol) in 12 mL of hexane, was added 6 equiv of $[Fe_2(CO)_9]$ (0.19 g, 0.54 mmol). The reaction mixture was thermolyzed at 50 °C for 24 h and cooled to room temperature. The solvent was removed in vacuo; the residue was extracted into hexane and passed through Celite. The filtrate was concentrated and kept at −40 °C to remove $[Fe_3(CO)_{12}]$. The mother liquor was concentrated, and the residue was chromatographed on silica gel TLC plates. Elution with a hexane/CH_2Cl_2 (7:3, v/v) mixture yielded red **2** (0.03 g, 36%), reddish brown **3** (0.015 g, 14%), and $[(\mu_3\text{-}BH)(Cp^*TaCO)_2(\mu\text{-}CO)\{Fe(CO)_3\}]$ (0.007 g, 9%).

2. ^{11}B NMR (22 °C, 128 MHz, C_6D_6): δ 84.7 (d, 1B), 53.9 (br, 2B), 36.5 (d, 2B). ^1H NMR (22 °C, 400 MHz, C_6D_6): δ 6.55 (partially collapsed quartet (pcq), $1BH_t$), 4.62 (pcq, $2BH_t$), 2.81 (pcq, $2BH_t$), 2.15 (s, 30H, 2Cp*), −3.73 (br, 2Ta−H−B). ^{13}C NMR (22 °C, 100 MHz, C_6D_6): δ 217.6, 206.1, 201.9 (CO), 115.0 (s, $C_5(CH_3)_5$), 12.9 (s, $C_5(CH_3)_5$). IR (hexane) ν/cm^{-1} 2510w, 2498w (BH_t), 2024s, 1996s, 1966s (CO). MS (FAB) P^+(max): m/z 973. Elem anal. Calcd for $C_{26}H_{37}B_5Fe_2O_6Ta_2$: C, 32.09; H, 3.83. Found: C, 33.19; H, 3.61.

3. ^{11}B NMR (22 °C, 128 MHz, C_6D_6): δ 87.8 (br, 1B), 72.3 (br, 1B), 48.7 (d, 1B), 9.4 (br, 1B), −3.9 (br, 1B). ^1H NMR (22 °C, 400 MHz, C_6D_6): δ 5.85 (pcq, $1BH_t$), 3.78 (pcq, $1BH_t$), 3.70 (pcq, $1BH_t$), 3.63 (pcq, $1BH_t$), 1.68 (s, 15H, Cp*), 1.59 (s, 15H, Cp*), −10.42 (br, 1Ta−H−B), −11.39 (br, 1Ta−H−B), −13.81 (br, 1Ta−H−B), −17.08 (s, 1Ta−H−Fe), −19.54 (s, 1Ta−H−Fe). ^{13}C NMR (22 °C, 100 MHz, C_6D_6): δ 218.2, 200.1 (CO), 108.3, 107.7 (s, $C_5(CH_3)_5$), 10.9, 10.7 (s, $C_5(CH_3)_5$). IR (hexane) ν/cm^{-1} 2489w (BH_t), 2032s, 1994s, 1938s (CO). MS (FAB) P^+(max): m/z 1254.

X-ray Structure Determination. Crystallographic information data for **2** and **3** are listed in Table 1. Crystal data for **2** were collected and integrated using a Oxford Diffraction XALIBUR-S CCD system

Table 1. Crystallographic Data and Structure Refinement Information for 2 and 3

	2	3
empirical formula	$C_{26}H_{37}B_5Fe_2O_6Ta_2$	$C_{35}H_{53}B_5Fe_4O_{12}Ta_2$
fw	973.21	1305.12
crystal system	triclinic	triclinic
space group	$P\bar{1}$	$P\bar{1}$
a (Å)	9.7195(2)	15.375(2)
b (Å)	11.9548(3)	16.931(3)
c (Å)	14.9240(3)	18.227(3)
α (deg)	91.659(2)	84.651(10)
β (deg)	92.388(2)	81.032(10)
γ (deg)	113.952(2)	89.855(10)
V (Å^3)	1581.38(6)	4666.0(13)
Z	2	4
D_{calc} (g/cm^3)	2.044	1.858
$F(000)$	928	2536
μ (mm^{-1})	7.832	5.934
crystal size (mm)	0.28 × 0.23 × 0.19	0.20 × 0.15 × 0.15
θ range (deg)	3.39−25.00	1.14−25.00
no. of total refins collected	11 242	88 914
no. of unique refins [$I > 2\sigma(I)$]	5561	16 425
max and min transmn	0.3176 and 0.2177	0.49 and 0.42
data/restraints/param	5561/0/408	16 425/28/1115
GOF on F^2	0.995	1.170
final R indices [$I > 2\theta(I)$]	R1 = 0.0186	R1 = 0.0245
	wR2 = 0.0446	wR2 = 0.0754
R indices (all data)	R1 = 0.0217	R1 = 0.0331
	wR2 = 0.0454	wR2 = 0.0860
largest difference in peak and hole (e/Å^3)	1.043 and −0.702	1.571 and −0.566

dx.doi.org/10.1021/ic102235p |*Inorg. Chem.* 2011, 50, 2445–2449

equipped with graphite-monochromated Mo Kα radiation (λ = 0.710 73 Å) at 150 K. The crystal data for **3** were collected and integrated using a Bruker AXS Kappa Apex2 CCD diffractometer, with graphite-monochromated Mo Kα (λ = 0.710 73 Å) radiation at 173 K. The structures were solved by heavy-atom methods using *SHELXS-97* or *SIR92*[33] and refined using *SHELXL-97* (Sheldrick, G. M., University of Göttingen, Göttingen, Germany).[34,35]

■ ASSOCIATED CONTENT

Supporting Information. X-ray crystallographic files in CIF format for **2** and **3**. This material is available free of charge via the Internet at http://pubs.acs.org.

■ AUTHOR INFORMATION

Corresponding Author
*E-mail: sghosh@iitm.ac.in. Fax: (+91) 44 2257 4202.

■ ACKNOWLEDGMENT

Generous support of the Department of Science and Technology, New Delhi, India (Project SR/S1/IC-19/2006), is gratefully acknowledged. S.K.B. and K.G. thank the University Grants Commission and Council of Scientific and Industrial Research, India, respectively, for Research Fellowships. We thank Shaikh M. Mobin for X-ray crystallography analysis. We also thank Mass Lab, SAIF, CDRI, Lucknow, India, for FAB mass analysis.

■ REFERENCES

(1) (a) Kennedy, J. D. *Prog. Inorg. Chem.* **1984**, *32*, 519–679. (b) Kennedy, J. D. *Prog. Inorg. Chem.* **1986**, *36*, 211–434.(c) Gilbert, K. B.; Boocock, S. K.; Shore, S. G. In *Comprehensive Organometallic Chemistry*; Wilkinson, G., Abel, E. W., Stone, F. G. A., Eds.; Pergamon: New York, 1982; Part 6, Chapter 41, pp 879−945. (d) Grimes, R. N. In *Comprehensive Organometallic Chemistry*; Wilkinson, G., Abel, E. W., Stone, F. G. A., Eds.; Pergamon: New York, 1982; Part 1, Chapter 5.5, pp 459−453.

(2) (a) Barton, L.; Srivastava, S. K. In *Comprehensive Organometallic Chemistry II*; Wilkinson, G., Abel, E. W., Stone, F. G. A., Eds.; Pergamon: New York, 1995; Vol. 1, Chapter 8, pp 275−373. (b) Grimes, R. N. In *Comprehensive Organometallic Chemistry II*; Wilkinson, G., Abel, E. W., Stone, F. G. A., Eds.; Pergamon: New York, 1995; Vol. 1, Chapter 9, pp 374−431. (c) Grimes, R. N. *Chem. Rev.* **1992**, *92*, 251–268. (d) Saxena, A. K.; Hosmane, N. S. *Chem. Rev.* **1993**, *93*, 1081–1124.

(3) Wade, K. *Adv. Inorg. Chem. Radiochem.* **1976**, *18*, 1–66.

(4) Mingos, D. M. P.; Wales, D. J. *Introduction to Cluster Chemistry*; Prentice Hall: New York, 1990.

(5) Wang, X.; Sabat, M.; Grimes, R. N. *Organometallics* **1995**, *14*, 4668–4675.

(6) Fehlner, T. P. In *Electron Deficient Boron and Carbon Clusters*; Olah, G. A., Wade, K., Williams, R. E., Eds.; Wiley: New York, 1991; p 287.

(7) (a) Bose, S. K.; Geetharani, K.; Varghese, B.; Mobin, S. M.; Ghosh, S. *Chem.—Eur. J.* **2008**, *14*, 9058–9064. (b) Bose, S. K.; Geetharani, K.; Ramkumar, V.; Mobin, S. M.; Ghosh, S. *Chem.—Eur. J.* **2009**, *15*, 13483–13490. (c) Geetharani, K.; Bose, S. K.; Varghese, B.; Ghosh, S. *Chem.—Eur. J.* **2010**, *16*, 11357–11366.

(8) (a) Bose, S. K.; Geetharani, K.; Ramkumar, V.; Varghese, B.; Ghosh, S. *Inorg. Chem.* **2010**, *49*, 2881–2888. (b) Bose, S. K.; Geetharani, K.; Varghese, B.; Ghosh, S. *Inorg. Chem.* **2010**, *49*, 6375–6377.

(9) Dhayal, R. S.; Chakrahari, K. K. V.; Varghese, B.; Mobin, S. M.; Ghosh, S. *Inorg. Chem.* **2010**, *47*, 7741–7747.

(10) Sahoo, S.; Mobin, S. M.; Ghosh, S. *J. Organomet. Chem.* **2010**, *695*, 945–949.

(11) Housecroft, C. E. *Boranes and Metalloboranes*; Ellis Horwood: Chichester, U.K., 1990.

(12) *The Chemistry of Metal Cluster Complexes*; Shriver, D. F., Kaesz, H. D., Adams, R. D., Eds.; VCH: New York, 1990.

(13) Lei, X.; Shang, M.; Fehlner, T. P. *Organometallics* **1998**, *17*, 1558–1563.

(14) Lei, X.; Shang, M.; Fehlner, T. P. *Chem. Commun.* **1999**, 933–934.

(15) (a) Ghosh, S.; Beatty, A. M.; Fehlner, T. P. *Angew. Chem., Int. Ed.* **2003**, *42*, 4678–4680. (b) Ghosh, S.; Fehlner, T. P.; Beatty, A. M. *Chem. Commun.* **2005**, 3080–3082. (c) Ghosh, S.; Shang, M.; Fehlner, T. P. *J. Am. Chem. Soc.* **1999**, *121*, 7451–7452.

(16) Vinitskii, D. M.; Lagun, V. L.; Solntsev, K. A.; Kuznetsov, N. T.; Marushkin, K. N.; Janousek, J.; Base, K.; Stibr, B. *Russ. J. Inorg. Chem.* **1984**, *29*, 984.

(17) Venable, T. L.; Grimes, R. N. *Inorg. Chem.* **1982**, *21*, 887–895.

(18) Bould, J.; Rath, N. P.; Fang, H.; Barton, L. *Inorg. Chem.* **1996**, *35*, 2062–2069.

(19) Pisareva, I. V.; Dolgushin, F. M.; Yanovsky, A. I.; Balagurova, E. V.; Petrovskii, P. V.; Chizhevsky, I. T. *Inorg. Chem.* **2001**, *40*, 5318–5319.

(20) De Montigny, F.; Macias, R.; Noll, B. C.; Fehlner, T. P. *Angew. Chem., Int. Ed.* **2006**, *45*, 2119–2122.

(21) Rivard, E.; Steiner, J.; Fettinger, J. C.; Giuliani, J. R.; Augustine, M. P.; Power, P. P. *Chem. Commun.* **2007**, 4919–4921.

(22) (a) Churchill, M. R.; Wasserman, H. J. *Inorg. Chem.* **1982**, *21*, 226–230. (b) Campbell, G. C.; Canich, J. A. M.; Cotton, F. A.; Duraj, S. A.; Haw, J. F. *Inorg. Chem.* **1986**, *25*, 287–290. (c) Belmonte, P. A.; Cloke, F. G. N.; Schrock, R. R. *J. Am. Chem. Soc.* **1983**, *105*, 2643–2650.

(23) Adams, R. D.; Chen, G.; Tanner, J. T.; Yin, J. *Organometallics* **1990**, *9*, 1240–1245.

(24) Knoll, K.; Fässler, T.; Huttner, G. *J. Organomet. Chem.* **1987**, *332*, 309–320.

(25) Maxwell, W. M.; Sinn, E.; Grimes, R. N. *J. Am. Chem. Soc.* **1976**, *98*, 3490–3495.

(26) Barker, G. K.; Garcia, M. P.; Green, M.; Stone, F. G. A.; Welch, A. J. *J. Chem. Soc., Dalton Trans.* **1982**, 1679–1686.

(27) Curtis, M. A.; Houser, E. J.; Sabat, M.; Grimes, R. N. *Inorg. Chem.* **1998**, *37*, 102–111.

(28) Wade, K. *J. Chem. Soc., Chem. Commun.* **1971**, 792–793.

(29) (a) Williams, R. E. *Inorg. Chem.* **1971**, *10*, 210–214. (b) Mingos, D. M. P. *J. Chem. Soc., Chem. Commun.* **1983**, 706–708. (c) Mingos, D. M. P. *Acc. Chem. Res.* **1984**, *17*, 311–319. (d) Mingos, D. M. P.; Johnston, R. L. *Struct. Bonding (Berlin)* **1987**, *68*, 31.

(30) (a) Mingos, D. M. P. *Nat. Phys. Sci.* **1972**, *236*, 99–102. (b) Mingos, D. M. P.; Forsyth, M. I. *J. Chem. Soc., Dalton Trans.* **1977**, 610–616.

(31) (a) Pipal, J. R.; Grimes, R. N. *Inorg. Chem.* **1977**, *16*, 3255–3262. (b) Venable, T. L.; Sinn, E.; Grimes, R. N. *Inorg. Chem.* **1982**, *21*, 904–908. (c) Bullick, H. J.; Grebenik, P. D.; Green, M. L. H.; Hughes, A. K.; Leach, J. B.; Mountford, P. *J. Chem. Soc., Dalton Trans.* **1994**, 3337–3342. (d) Bould, J.; Rath, N. P.; Barton, L. *Organometallics* **1995**, *14*, 2119–2122. (e) Bould, J.; Rath, N. P.; Barton, L. *J. Chem. Soc., Chem. Commun.* **1995**, 1285–1286. (f) Lei, X.; Shang, M.; Fehlner, T. P. *J. Am. Chem. Soc.* **1999**, *121*, 1275–1287.

(32) Ryschkewitsch, G. E.; Nainan, K. C. *Inorg. Synth.* **1974**, *15*, 113–114.

(33) Altomare, A.; Cascarano, G.; Giacovazzo, C.; Guagliardi, A. *J. Appl. Crystallogr.* **1993**, *26*, 343–350.

(34) Sheldrick, G. M. *SHELXS-97*; University of Göttingen: Göttingen, Germany, 1997.

(35) Sheldrick, G. M. *SHELXL-97*; University of Göttingen: Göttingen, Germany, 1997.